

# Supplementary Materials for “The benefits of ambitious short-term targets when decarbonising the coupled electricity and heating energy system in Europe”

## 1. Historical Greenhouse Gases emissions in the European Union

The carbon budget from now onwards for the generation of electricity and the supply of heating in residential and services sector in Europe accounts for 21 GtCO<sub>2</sub>. It has been estimated based on a global carbon budget of 800 GtCO<sub>2</sub> to avoid temperature increments above 2°C relative to preindustrial period with a probability of greater than 66% [1, 2]. The global budget is assumed to be split among regions according to a constant per-capita ratio which translates into a 6% share for Europe [3]. Out of the total emissions in Europe, the ratio corresponding to electricity and heating is considered constant and equal to present values. In 2017, electricity generation and heating in the residential and services sector emitted 1.56 GtCO<sub>2</sub> which represents 43.5% of European emissions, [4] and Figure 1.

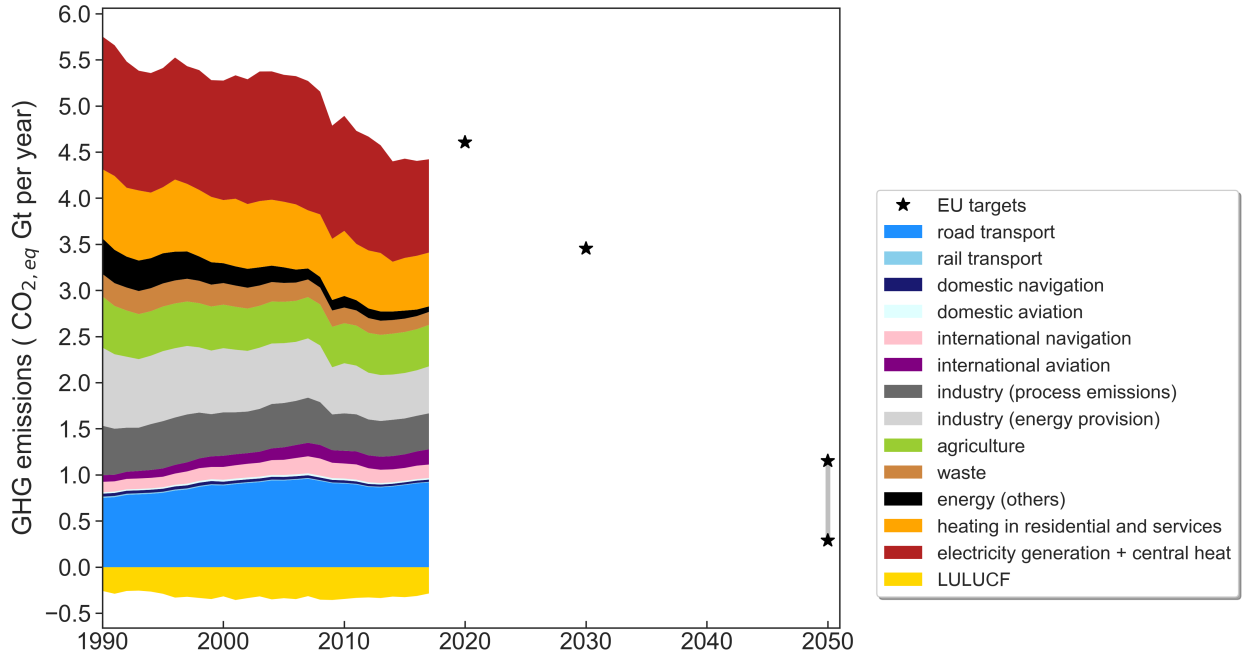


Figure 1: Sectoral distribution of historical emissions in the European Union [4]. The stars indicate committed EU reduction targets.

## 2. CO<sub>2</sub> restriction paths with equivalent budget

The  $B=21$  GtCO<sub>2</sub> budget can be utilised following different transition paths. One option consists in assuming a linear CO<sub>2</sub> restriction path. Emissions will then reach zero in  $t_f$

$$t_f = t_0 + \frac{2B}{e_0} \quad (1)$$

where  $t_0=2020$ , and  $e_0$  represents the carbon emissions from electricity and heating sector in 2020, which are assumed to be the same as in 2017.

Alternatively, emissions can be assumed to follow a path defined by one minus the cumulative distribution function ( $CDF_\beta$ ) of a beta distribution in which  $\beta_1 = \beta_2$ .

$$\begin{aligned} e(t) &= e_0(1 - CDF_\beta(t)) \\ CDF_\beta(t) &= \int_{-\infty}^t PDF_\beta(t) dt \\ PDF_\beta(t) &= \frac{\Gamma(\beta_1 + \beta_2)}{\Gamma(\beta_1) + \Gamma(\beta_2)} t^{\beta_1-1} (1-t)^{\beta_2-1} \end{aligned} \quad (2)$$

where  $\Gamma$  is the gamma function. The cumulative emissions fulfil  $\int_{t_0}^{\infty} e(t) dt = B$ .

The third option considered for the transition path is an exponential decay, following Raupach *et al.* [3]. In that case, emissions evolve as:

$$e(t) = e_0(1 + (r + m)t)e^{-mt} \quad (3)$$

where  $r$  is the initial linear growth rate, which here is assumed to be  $r=0$ , and the decay parameter  $m$  is determined by imposing the integral of the path to be equal to the budget.

$$\begin{aligned} B &= \int_{t_0}^{\infty} e_0(1 + (r + m)t)e^{-mt} dt \\ m &= \frac{1 + \sqrt{1 + \frac{rB}{e_0}}}{\frac{B}{e_0}} \end{aligned} \quad (4)$$

Although the exponential decay path approaches asymptotically to zero, we assume here that  $e(2050) = 0$ . By doing that, the final point of the different transition paths is equivalent and all of them achieve net-zero emissions by 2050.

3. Historical evolution of CO<sub>2</sub> emissions from heating supply in residential and services sector in European countries
4. Power plants in operation in Europe
5. Historical build rates for solar photovoltaics in European countries
6. Transition paths cautious and last-minute. Additional results

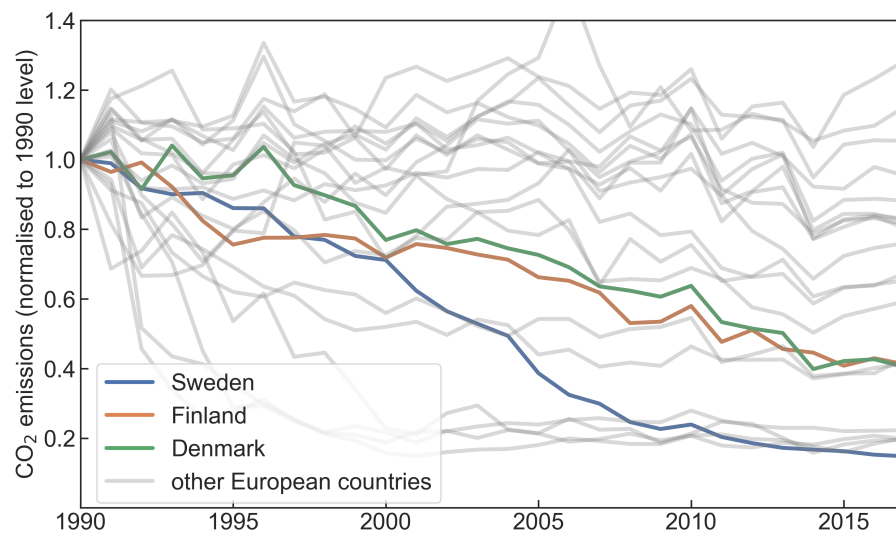


Figure 2: Historical CO<sub>2</sub> emissions from heating in residential and services sector [4].

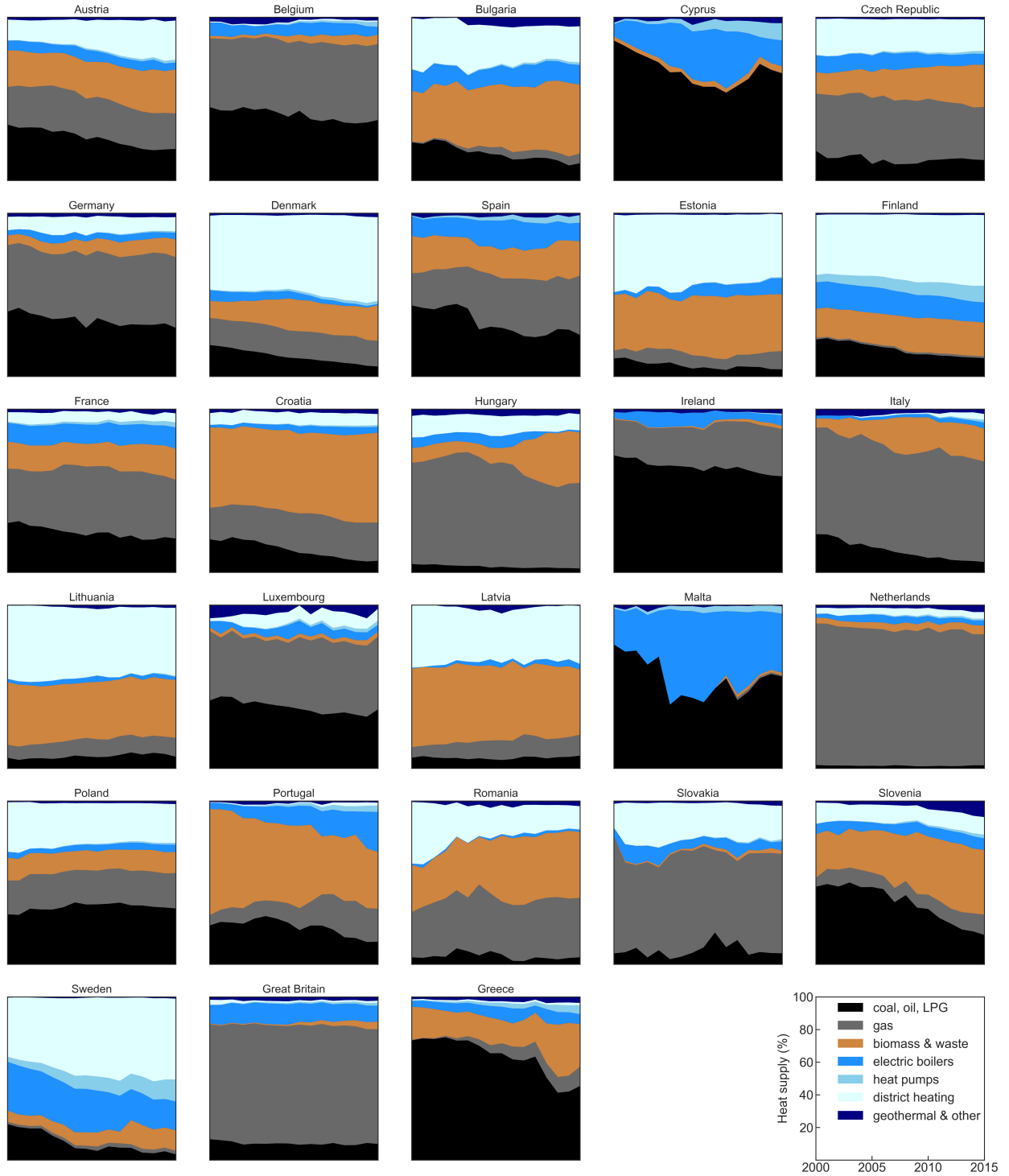


Figure 3: Historical share of technologies used to supply heating in residential and services sector [5].

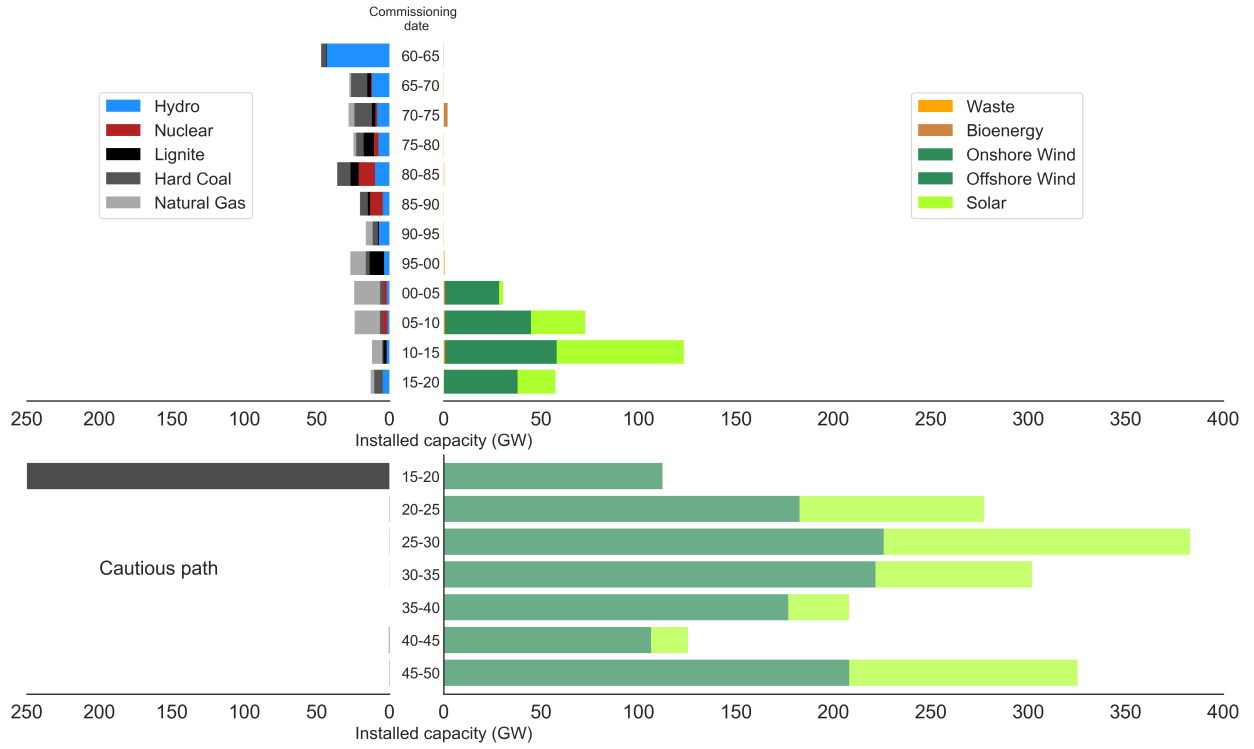


Figure 4: Age distribution of European power plants in operation [6, 7]

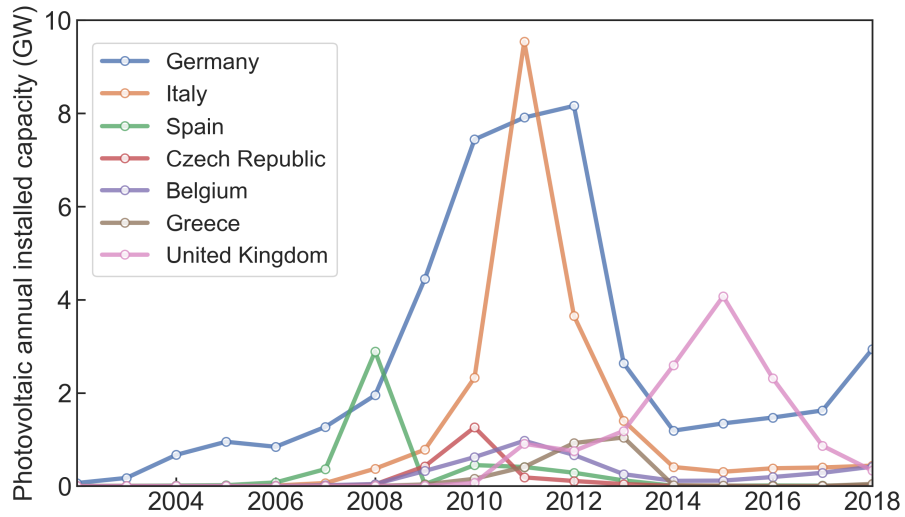


Figure 5: Photovoltaic annual build rates for those European countries with a prominent peak [7]. The sharp increase and subsequent decrease in the installation rates were caused by country-specific successive changes in the regulatory frameworks. See for instance [8, 9].

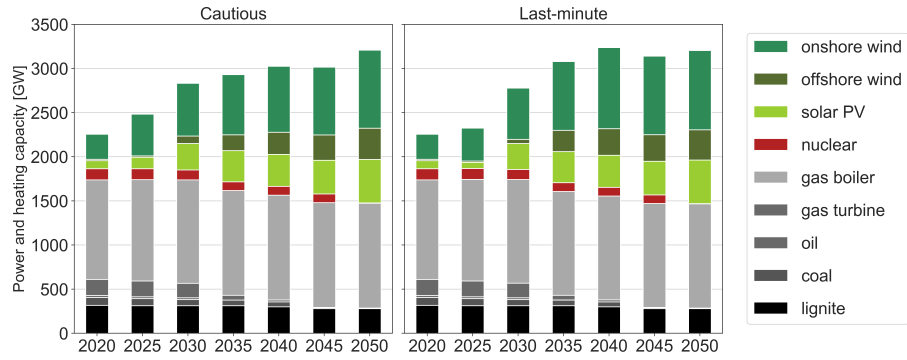


Figure 6: Installed capacities for different technologies throughout transition paths cautious and last-minute shown in Fig. 1 in the main text.

Figure 7: Primary energy in every country in 2050. (left) Cautious transition path, (right) Greenfield optimization for 2050.

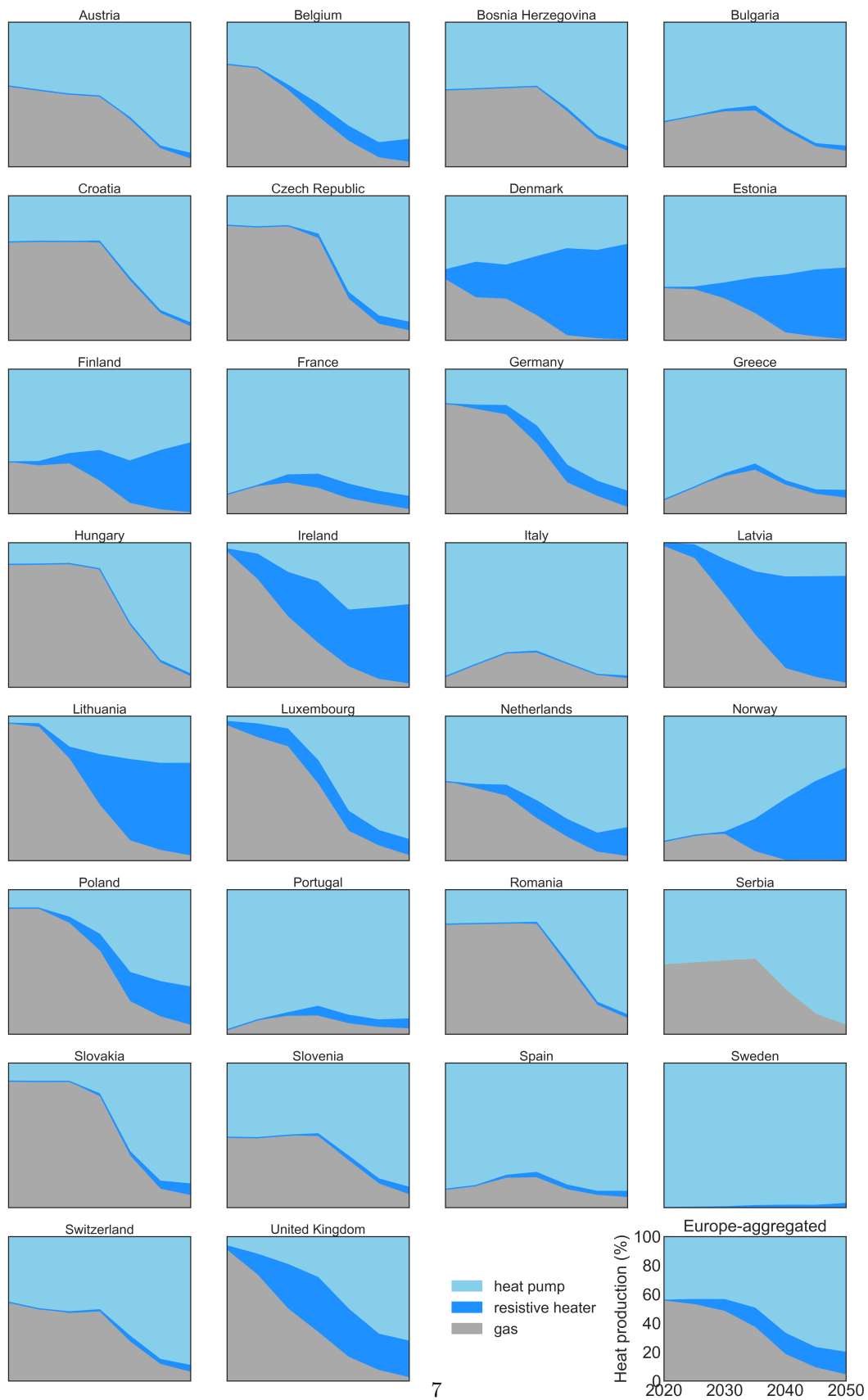


Figure 8: Evolution of technologies used to supply heating in residential and services sector in the cautious path.

## 7. Model description

In every time step, the optimisation objective, that is, the total annualised system cost is calculated as:

$$\min_{\substack{G_{n,s}, E_{n,s}, \\ F_\ell, g_{n,s,t}}} \left[ \sum_{n,s} c_{n,s} \cdot G_{n,s} + \sum_{n,s} \hat{c}_{n,s} \cdot E_{n,s} + \sum_{\ell} c_\ell \cdot F_\ell + \sum_{n,s,t} o_{n,s,t} \cdot g_{n,s,t} \right] \quad (5)$$

where  $c_{n,s}$  are the fixed annualised costs for generator and storage power capacity  $G_{n,s}$  of technology  $s$  in every bus  $n$ ,  $\hat{c}_{n,s}$  are the fixed annualised costs for storage energy capacity  $E_{n,s}$ ,  $c_\ell$  are the fixed annualised costs for bus connectors  $F_\ell$ , and  $o_{n,s,t}$  are the variable costs (which in some cases include CO<sub>2</sub> tax), for generation and storage dispatch  $g_{n,s,t}$  in every hour  $t$ . Bus connectors  $\ell$  include transmission lines but also converters between the buses implemented in every country (see Figure ??), for instance, heat pumps that connect the electricity and heating bus.

The optimisation of the system is subject to several constraints. First, hourly demand  $d_{n,t}$  in every bus  $n$  must be supplied by generators in that bus or imported from other buses.  $f_{\ell,t}$  represents the energy flow on the link  $\ell$  and  $\alpha_{n,\ell,t}$  indicates both the direction and the efficiency of flow on the bus connectors.  $\alpha_{n,\ell,t}$  can be time dependent such as in the case of heat pumps whose conversion efficiency depends on the ambient temperature.

$$\sum_s g_{n,s,t} + \sum_\ell \alpha_{n,\ell,t} \cdot f_{\ell,t} = d_{n,t} \leftrightarrow \lambda_{n,t} \quad \forall n, t \quad (6)$$

The Lagrange multiplier  $\lambda_{n,t}$ , also known as Karun-Kush-Tucker (KKT), associated with the demand constraint indicates the marginal price of the energy carrier in the bus  $n$ , *e.g.*, local marginal electricity price in the electricity bus.

Second, the maximum power flowing through the links is limited by their maximum physical capacity  $F_\ell$ . For transmission links,  $\underline{f}_{\ell,t} = -1$  and  $\bar{f}_{\ell,t} = 1$ , which allows both import and export between neighbouring countries. For a unidirectional converter *e.g.*, a heat resistor,  $\underline{f}_{\ell,t} = 0$  and  $\bar{f}_{\ell,t} = 1$  since a heat resistor can only convert electricity into heat.

$$\underline{f}_{\ell,t} \cdot F_\ell \leq f_{\ell,t} \leq \bar{f}_{\ell,t} \cdot F_\ell \quad \forall \ell, t. \quad (7)$$

For interconnecting transmission lines, the lengths  $l_\ell$  are set by the distance between the geographical mid-points of each country, so that some of the transmission within each country is also reflected in the optimisation. A factor of 25% is added to the line lengths to account for the fact that transmission lines cannot be placed as the crow flies due to land use restriction. For the transmission lines capacities  $F_\ell$ , a safety margin of 33% of the installed capacity is used to satisfy n-1 requirements [10].

Third, for every hour the maximum capacity that can provide a generator or storage is bounded by the product between installed capacity  $G_{n,s}$  and availabilities  $\underline{g}_{n,s,t}$ ,  $\bar{g}_{n,s,t}$ . For instance, for solar generators  $\underline{g}_{n,s,t}$  is zero and  $\bar{g}_{n,s,t}$  refers to the capacity factor at time  $t$

$$\underline{g}_{n,s,t} \cdot G_{n,s} \leq g_{n,s,t} \leq \bar{g}_{n,s,t} \cdot G_{n,s} \quad \forall n, s, t. \quad (8)$$

The maximum power capacity for generators is limited by potentials  $\bar{G}_{n,s}$  that are estimated taking into account physical and environmental constraints:

$$0 \leq G_{n,s} \leq \bar{G}_{n,s} \quad \forall n, s. \quad (9)$$



The storage technologies have a charging efficiency  $\eta_{in}$  and rate  $g_{n,s,t}^+$ , a discharging efficiency  $\eta_{out}$  and rate  $g_{n,s,t}^-$ , possible inflow  $g_{n,s,t,\text{inflow}}$  and spillage  $g_{n,s,t,\text{spillage}}$ , and standing loss  $\eta_0$ . The state of charge  $e_{n,s,t}$  of every storage has to be consistent with charging and discharging in every hour and is limited by the energy capacity of the storage  $E_{n,s}$ . It should be remarked that the storage energy capacity  $E_{n,s}$  can be optimised independently of the storage power capacity  $G_{n,s}$ .

$$\begin{aligned} e_{n,s,t} &= \eta_0 \cdot e_{n,s,t-1} + \eta_{in} |g_{n,s,t}^+| - \eta_{out}^{-1} |g_{n,s,t}^-| \\ &\quad + g_{n,s,t,\text{inflow}} - g_{n,s,t,\text{spillage}} , \\ 0 &\leq e_{n,s,t} \leq E_{n,s} \quad \forall n, s, t . \end{aligned} \quad (10)$$

So far, equations (6) to (10) represent mainly technical constraints but additional constraints can be imposed to bound the solution.

The interconnecting transmission expansion can be limited by a global constraint

$$\sum_{\ell} l_{\ell} \cdot F_{\ell} \leq \text{CAP}_{LV} \quad \leftrightarrow \quad \mu_{LV} , \quad (11)$$

where the sum of transmission capacities  $F_{\ell}$  multiplied by the lengths  $l_{\ell}$  is bounded by a transmission volume cap  $\text{CAP}_{LV}$ . In this case, the Lagrange/KKT multiplier  $\mu_{LV}$  represents the shadow price of a marginal increase in transmission volume.

The maximum  $\text{CO}_2$  allowed to be emitted by the system  $\text{CAP}_{\text{CO}_2}$  can be imposed through the constraint

$$\sum_{n,s,t} \varepsilon_s \frac{g_{n,s,t}}{\eta_{n,s}} + \sum_{n,s} \varepsilon_s (e_{n,s,t=0} - e_{n,s,t=T}) \leq \text{CAP}_{\text{CO}_2} \quad \leftrightarrow \quad \mu_{\text{CO}_2} \quad (12)$$

where  $\varepsilon_s$  represents the specific emissions in  $\text{CO}_2$ -tonne-per-MWh<sub>th</sub> of the fuel  $s$ ,  $\eta_{n,s}$  the efficiency and  $g_{n,s,t}$  the generators dispatch. In this case, the Lagrange/KKT multiplier represents the shadow price of  $\text{CO}_2$ , *i.e.*, the additional price that should be added for every unit of  $\text{CO}_2$  to achieve the  $\text{CO}_2$  reduction target in an open market.

## 8. Sectors description and data

### 8.1. Electricity sector

Hourly electricity demand for every country corresponding to 2015 is retrieved from EU Network Transmission System Operators of Electricity (ENTSO-E) via the convenient dataset prepared by the Open Power System Data (OPSD) initiative [11]. In every country, electricity can be generated by solar PV, onshore wind, offshore wind, Open Cycle Gas Turbines (OCGT), Combined Cycle Gas Turbines (CCGT), coal, lignite, and nuclear power plants and CHP units, with the costs, lifetimes and efficiencies shown in Table 2. Time series representing the hourly capacity factors for solar PV were obtained by converting weather data into solar electricity generation, assuming a uniform capacity layout across every country. Details on the conversion and aggregation methodology can be found in [12], the complete time series dataset is available in [10.5281/zenodo.1321809](https://doi.org/10.5281/zenodo.1321809). CHP units are modelled as extraction condensing units, the feasible space representing the possible combinations of power and heat outputs is included as a constraint in the model, as detailed in [13].

**TODO: Describe onshore/offshore time series and maximum capacities.**

**TODO: Describe maximum capacities.**

The transmission links between countries are assumed to be high-voltage direct current (HVDC) connections. For 2020 and 2030, the capacities corresponds to the values assumed in the ENTSOE Ten-Year Network Development Plan (TNYDP), see Table 1 and [14]. The values for 2025 are interpolated assuming

a liner capacity expansion between 2020 and 2030 for every link. For years from 2035 onwards, capacities are optimized together with the rest of the system components using 2030 values as lower boundary. **TODO: Describe other scenarios**

For conventional technologies, *i.e.* OCGT, CCGT, coal, lignite, nuclear and CHP, installed capacities in every country in 2020 and commissioning dates are retrieved from [6]. A two-step method was implemented to fill commissioning date for power plants whose data was missing. First, for units larger than 50 MW, commissioning date has been searched and manually added. Then, for smaller units, a Kernel Density Estimation (KDE) approach is used. *I.e.*, for every technology and country, the units with available data are used to create a distribution, which is then used to assign an estimated commissioning date for those units with missing data. For solar PV, the installed capacities in 2020 and the installation dates were obtained by processing annual installed capacities statistics from [7]. For offshore and onshore wind, capacities and age are retrieved from [15].

**TODO: Include figure with the sectors included.**

## 8.2. Heating sector

Annual heat demand for every country are retrieved from [16]. They are converted into hourly heat demand based on the population-weighted [17] Heating Degree Hour (HDH), that is, heating is assumed to be proportional to the difference between ambient temperature and a threshold temperature. 17°C is assumed as threshold temperature. **TODO: Change to daily profiles?** In high-density population areas, heating can be supplied by central heat pumps, heat resistors and gas boilers, as well as by CPH and **solar collectors**. In low-density population areas, heating can be supplied by individual heat pumps, heat resistors and gas boilers. Costs, lifetimes, and efficiencies of the different technologies are included in Table 2.

**TODO: Describe temperature-dependent efficiency of heat pumps. Include formula for LCOE estimation. Describe reference and method for existing heating capacities. Describe hypotheses on biomass and assumptions from JRC-ENSURES. Describe path of deployment of district heating. Describe path of electrification of transport.**

## 9. Cost assumptions

Figure 9: Cost evolution assumed for the different technologies.

## 10. References

- [1] C. Figueres, H. J. Schellnhuber, G. Whiteman, J. Rockström, A. Hobley, S. Rahmstorf, [Three years to safeguard our climate](#), Nature News 546 (7660) 593. doi:10.1038/546593a.  
URL <http://www.nature.com/news/three-years-to-safeguard-our-climate-1.22201>
- [2] G. Peters, How much carbon dioxide can we emit?  
URL <https://cicero.oslo.no/en/posts/climate/how-much-carbon-dioxide-can-we-emit>
- [3] M. R. Raupach, S. J. Davis, G. P. Peters, R. M. Andrew, J. G. Canadell, P. Ciais, P. Friedlingstein, F. Jotzo, D. P. Vuuren, C. L. Quéré, [Sharing a quota on cumulative carbon emissions](#), Nature Climate Change 4 (10) (2014) 873–879. doi:10.1038/nclimate2384.  
URL <https://www.nature.com/articles/nclimate2384>
- [4] National emissions reported to the UNFCCC and to the EU Greenhouse Gas Monitoring Mechanism, EEA.  
URL <https://www.eea.europa.eu/data-and-maps/data/national-emissions-reported-to-the-unfccc-and-to-the-eu-greenhouse-gas>
- [5] L. Mantzos, T. Wiesenhal, N. Matei, S. Tchung-Ming, M. Rzsai, H. P. Russ, A. Soria, [JRC-IDEES: Integrated Database of the European Energy Sector](#) doi:10.2760/182725.  
URL <http://www.sciencedirect.com/science/article/pii/S0360544216310295>
- [6] powerplantmatching.  
URL <https://github.com/FRESNA/powerplantmatching>
- [7] Renewable Capacity Statistics 2019, IRENA.  
URL <https://www.irena.org/publications/2019/Mar/Renewable-Capacity-Statistics-2019>

Table 1: Transmission capacities (MW) for interconnections [14].

Link	2020	2030	Link	2020	2030	Link	2020	2030
AL-GR	250	250	FI-EE	1000	1000	LU-FR	0	0
AL-ME	350	350	FI-NO	0	0	LV-EE	1600	1600
AL-MK	200	200	FI-SE	2300	2800	LV-LT	1200	1800
AL-RS	760	760	FR-BE	4300	4300	ME-AL	350	350
AT-CH	1700	1700	FR-CH	3700	3700	ME-BA	400	400
AT-CZ	1000	1000	FR-DE	3000	4800	ME-IT	1200	1200
AT-DE	5000	7500	FR-ES	5000	8000	ME-RS	1000	1000
AT-HU	1200	1200	FR-GB	5400	5400	MK-AL	200	200
AT-IT	555	1655	FR-IE	0	700	MK-BG	150	150
AT-SI	1200	1200	FR-IT	4350	4350	MK-GR	400	400
BA-HR	1344	1844	FR-LU	380	380	MK-RS	1050	1050
BA-ME	500	500	GB-BE	1000	1000	NI-GB	80	500
BA-RS	1100	1100	GB-DK	1400	1400	NI-IE	1100	1100
BE-DE	1000	1000	GB-FR	5400	5400	NL-BE	2400	2400
BE-FR	2800	2800	GB-IE	500	500	NL-DE	4450	5000
BE-GB	1000	1000	GB-IS	0	0	NL-DK	700	700
BE-LU	1080	1080	GB-NI	500	500	NL-GB	1000	1000
BE-NL	2400	2400	GB-NL	1000	1000	NL-NO	700	700
BG-GR	1728	1728	GB-NO	1400	1400	NO-DE	1400	1400
BG-MK	530	530	GR-AL	250	250	NO-DK	1640	1640
BG-RO	1400	1400	GR-BG	1032	1032	NO-FI	0	0
BG-RS	600	600	GR-CY	2000	2000	NO-GB	1400	1400
CH-AT	1700	1700	GR-IT	500	500	NO-NL	700	700
CH-DE	4700	4700	GR-MK	350	350	NO-SE	3695	3695
CH-FR	1300	1300	HR-BA	1312	1812	PL-CZ	600	600
CH-IT	6240	6240	HR-HU	2000	2000	PL-DE	3000	3000
CY-GR	2000	2000	HR-IT	0	0	PL-DK	0	0
CZ-AT	1200	1200	HR-RS	600	600	PL-LT	1000	1000
CZ-DE	2100	2600	HR-SI	2000	2000	PL-PL	5000	5000
CZ-PL	500	500	HU-AT	800	800	PL-SE	600	600
CZ-SK	2100	2100	HU-HR	2000	2000	PL-SK	990	990
DE-AT	5000	7500	HU-RO	1300	1300	PT-ES	3500	3500
DE-BE	1000	1000	HU-RS	600	600	RO-BG	1500	1500
DE-CH	3286	3286	HU-SI	1700	1700	RO-HU	1400	1400
DE-CZ	1500	2000	HU-SK	2000	2000	RO-RS	1450	1450
DE-DK	4000	4000	IE-FR	0	700	RS-AL	330	330
DE-FR	3000	4800	IE-GB	500	500	RS-BA	1200	1200
DE-LU	2300	2300	IE-NI	1100	1100	RS-BG	350	350
DE-NL	4450	5000	IS-GB	0	0	RS-HR	600	600
DE-NO	1400	1400	IT-AT	385	1385	RS-HU	600	600
DE-PL	2000	2000	IT-CH	3860	3860	RS-ME	1100	1100
DE-SE	615	1315	IT-FR	2160	2160	RS-MK	950	950
DK-DE	4000	4000	IT-GR	500	500	RS-RO	1050	1050
DK-DK	1200	1200	IT-HR	0	0	SE-DE	615	1315
DK-GB	1400	1400	IT-IT	5750	5750	SE-DK	1980	1980
DK-NL	700	700	IT-ME	1200	1200	SE-FI	2400	3200
DK-NO	1640	1640	IT-SI	1380	1380	SE-LT	700	700
DK-PL	0	0	IT-TN	0	0	SE-NO	3995	3995
DK-SE	2440	2440	LT-LV	1500	2100	SE-PL	600	600
EE-FI	1016	1016	LT-PL	1000	1000	SI-AT	1200	1200
EE-LV	1600	1600	LT-SE	1700	700	SI-HR	2000	2000
ES-FR	5000	8000	LU-BE	700	700	SI-HU	2000	2000
ES-PT	4200	4200	LU-DE	2300	2300	SI-IT	1530	1530

- [8] [Photovoltaics Report](#), Tech. rep., Fraunhofer ISE (2019).  
URL <https://www.ise.fraunhofer.de/content/dam/ise/de/documents/publications/studies/Photovoltaics-Report.pdf>
- [9] M. Victoria, C. Gallego, I. Anton, G. Sala, [Past, Present and Future of Feed-in Tariffs in Spain: What are their Real Costs?](#), 27th European Photovoltaic Solar Energy Conference and Exhibition (2012) 4612–4616 [doi:10.4229/27thEUPVSEC2012-6CV.3.49](#).  
URL <http://www.eupvsec-proceedings.com/proceedings?paper=17736>
- [10] T. Brown, P. Schierhorn, E. Tröster, T. Ackermann, Optimising the european transmission system for 77% renewable electricity by 2030 10 (1) 3–9. [doi:10.1049/iet-rpg.2015.0135](#).
- [11] [Open Power System Data](#). 2018. Data Package Time series. Version 2018-03-13. (Primary data from various sources, for a complete list see URL).  
URL [https://data.open-power-system-data.org/time\\_series/2018-03-13/](https://data.open-power-system-data.org/time_series/2018-03-13/).
- [12] M. Victoria, G. B. Andresen, [Using validated reanalysis data to investigate the impact of the PV system configurations at high penetration levels in european countries](#), Progress in Photovoltaics: Research and Applications 27 (7) 576–592. [doi:10.1002/pip.3126](#).  
URL <https://onlinelibrary.wiley.com/doi/full/10.1002/pip.3126>
- [13] T. Brown, D. Schlachtberger, A. Kies, S. Schramm, M. Greiner, [Synergies of sector coupling and transmission reinforcement in a cost-optimised, highly renewable European energy system](#), Energy 160 (2018) 720–739. [doi:10.1016/j.energy.2018.06.222](#).  
URL <http://www.sciencedirect.com/science/article/pii/S036054421831288X>
- [14] [Ten-Year Network Development Plan 2016](#), ENTSOE.

Table 2: Cost assumption per technology and year.

Technology <sup>1</sup>	2020	2025	2030	2035	2040	2045	2050	source
Battery inverter								
Battery storage								
Coal power plant								
Combined heat and power								
Direct air capture								
Electric boiler								
Electrolysis								
Fuel cell								
Gas boiler central								
Gas boiler individual								
Heat pump central								
Heat pump individual								
High voltage direct current line								
Hot water tank central								
Hot water tank individual								
Hydro reservoir								
Hydrogen storage								
Lignite power plant								
Methanation								
Nuclear								
Offshore wind								
Oil power plant								
Onshore wind								
Open cycle gas turbine								
Pumped hydro storage								
Run of river								
Solar PV rooftop								
Solar PV utility								

<sup>1</sup> Sorted by alphabet.

Table 3: Efficiency, lifetime and FOM cost per technology, include references.

- URL <https://tyndp.entsoe.eu/maps-data/>
- [15] Wind energy database.  
URL <https://www.thewindpower.net/>
- [16] Deliverable 3.1: Profile of heating and cooling demand in 2015. Data Annex. Heat Roadmap Europe.  
URL [www.heatroadmap.eu](http://www.heatroadmap.eu)
- [17] Population density by NUTS 3 region.  
URL <https://data.europa.eu>